Separation and Purification Technology 146 (2015) 326–341

Contents lists available at ScienceDirect

Separation and Purification Technology

journal homepage: www.elsevier.com/locate/seppur

Screening of pervaporation membranes with the aid of conceptual models: An application to bioethanol production

María Angélica Sosa [a,1], Danilo Alexander Figueroa Paredes [a,1], Juan Carlos Basílico [b], Bart Van der Bruggen [c], José Espinosa [a,b,*]

[a] INGAR-CONICET, Avellaneda 3657, 3000 Santa Fe, Argentina
[b] Universidad Nacional del Litoral (UNL), Santiago del Estero 2829, 3000 Santa Fe, Argentina
[c] Department of Chemical Engineering, ProcESS – Process Engineering for Sustainable Systems, KU Leuven, W. de Croylaan 46, B-3001 Leuven, Belgium

ARTICLE INFO

Article history:
Received 7 January 2015
Received in revised form 30 March 2015
Accepted 3 April 2015
Available online 9 April 2015

Keywords:
Bioethanol production
Pervaporation
Distillation
Membrane performance
Conceptual modeling

ABSTRACT

In this paper, we assess the performance of a given hydrophobic membrane from the conceptual design of a hybrid process formed by the hydrophobic membrane itself and the separation train located downstream. To this end, a single pervaporation experiment with a model ethanol–water mixture is needed to estimate the minimum area requirement of the hydrophobic membrane. Short-cut methods, on the other hand, can be used to estimate the minimum number of stages and reflux ratio of the distillation column. Estimation of the minimum area requirement for a hydrophilic membrane, which is considered to overcome the azeotropic composition, requires the integration of a spatially one-dimensional isothermal mass transfer model of the unit until the desired biofuel purity is achieved in the corresponding retentate stream.

The idea behind the approach is that the performance of a given membrane must be measured taking into account the overall hybrid process given that the hydrophobic membrane itself performs only a part of the desired separation.

The hybrid process is then assessed on the basis of a cost estimate using the minimum membrane areas of the two membrane units together with minimum number of stages and minimum reflux ratio of the distillation column among other structural and operating variables.

The outcome allows for the screening of pervaporation membranes, and yields valuable insights into the nature of the process as well as the constraints that a hybrid process may face. Membranes can be assessed based on their overall process performance by this method; only the subset of membranes presenting the best economic figures can be considered for a further analysis.

1. Introduction

Pervaporation is a well-known membrane based separation process with major applications in the dehydration of organic solvents, particularly those which form azeotropes with water (such as ethanol and isopropanol). The first systematic work on pervaporation was done by Binning et al. [1] at American Oil in the 1950s. They explained the mass transfer process through thin plastic films in terms of the solution-diffusion mechanism and emphasized the commercial potential for separating azeotropes and several organic mixtures. The process was not commercialized until 1982 when GFT (Gesellschaft fuer TrennTechnik GmbH, Germany) installed the first commercial pervaporation plant to deal with alcohol dehydration [2]. GFT has since installed more than 100 such plants.

One of the key issues in bioethanol fermentation is the inhibition that the fermentative microorganism (yeast) experiences by the product itself. As a consequence, a rather low ethanol concentration is reached in the final fermentation broth [3]. Several authors pointed out that this problem could be overcome by the use of a solvent removal technology like hydrophobic pervaporation [4–8]. Moreover, the performance of the fermentation unit may be improved due to an increase in the concentration of viable yeast cells through water removal via pervaporation and the use of more concentrated substrate solutions [9]. Additional benefits emerging from the integration of the fermentation with a pervaporation unit would be the switching of the operating mode of

* Corresponding author. Tel.: +54 342 4555229.
E-mail address: destila@santafe-conicet.gov.ar (J. Espinosa).
[1] María Angélica Sosa and Danilo Alexander Figueroa Paredes contributed equally to this work.

http://dx.doi.org/10.1016/j.seppur.2015.04.001
1383-5866/

Nomenclature

A, A_{min}, a_{min}	membrane area (m^2), min = minimum
$a_{i,P}$	activity of component i in permeate
B	bottom flow rate (kmol/s)
D	distillate flow rate (kmol/s)
$E_{a,i}$	apparent activation energy of component i (J/mol)
EOS	equation of state
ΔT_{min}	minimum approach temperature in heat exchangers
Hyd+	hydrophilic
Hyd−	hydrophobic
J_i^{mass}	mass flux of component i through the membrane (g/(m^2 h))
J_i^{mol}	molar flux of component i through the membrane (kmol/(m^2 h))
L_F	feed flow rate leaving the fermentation unit (kmol/s)
$L_F^{infinite}$	36 kmol/s
L_R	retentate flow rate leaving the hydrophobic membrane (kmol/s)
LMTD	logarithmic mean temperature difference
M_i	molecular weight of component i
m_i^0	parameter for component i, mass-transfer model in Vier [41]
MINLP	mixed integer non-linear programming
N_i	parameter for component i, mass-transfer model in Vier [41]
NIST	National Institute of Standards and Technology
OC	overall cost (U$S/year)
OCp	overall cost of pervaporation unit (U$S/year)
OCvr	overall cost of vacuum-refrigeration system (U$S/year)
P_i^0	saturated vapor pressure of component i (kPa)
P_p	permeate pressure (kPa)
P^+	permeate flow rate leaving the hydrophilic membrane (kmol/s)
P^-	permeate flow rate leaving the hydrophobic membrane (kmol/s)
P_{high}	high operation pressure of the refrigeration cycle (kPa)
P_{low}	low operation pressure of the refrigeration cycle (kPa)
PSI	performance separation index
PSI_B	performance separation index for binary mixtures
PSI_M	performance separation index for multicomponent mixtures
R	universal gas constant (J/(mol K))
R, r	retentate flow rate leaving the hydrophilic membrane (kmol/s)
R_{min}	minimum reflux ratio of the distillation column
R_{op}	actual reflux ratio of the distillation column
T, T_{max}	temperature, max. working temp. of the hydrophilic membrane (K)
$T_{cooling}$	cooling temperature of the permeate stream
$T_{freezing}$	freezing point
x_B	mass or mole fraction of ethanol in B
x_D	mass or mole fraction of ethanol in D
x_L	mass or mole fraction of ethanol in the feed to the hydrophobic membrane
x_N	minimum feed composition for which a tangent pinch controls the separation
x_F	mass or mole fraction of ethanol in the feed to the column
x_{P+}	mass or mole fraction of ethanol in P^+
x_{P-}	mass or mole fraction of ethanol in P^-
x_P	feed pinch
x_R	mass or mole fraction of ethanol in R
x_{R-}	mass or mole fraction of ethanol in L_R
x_t	tangent pinch
x_i, y_i	retentate and permeate mole fractions in mass transfer models
$x_{ethanol}$, $y_{ethanol}$	ethanol liquid and vapor mole fractions in the diagram y versus x
VCRC	vapor-compression refrigeration cycle

Greek letters

α	selectivity factor
α_i	parameter for component i, mass-transfer model in Vier [41]
β	enrichment factor
γ_i	activity coefficient of component i
σ_{EtOH}^P	ethanol recovery in condensed permeate (%)

the fermentor from batch to continuous and the elimination of the beer column in the flowsheet of the conventional process [4,6].

For the production of biofuels, pervaporation can be applied to both the recovery of alcohols from fermentation broth and for the dehydration of the alcohols to meet fuel dryness specifications [9,10]. Huang et al. [11] performed a comprehensive review of feasible separation technologies in biorefineries. The mentioned authors include the hybrid process pervaporation–fermentation followed by ethanol dehydration via hydrophilic pervaporation among the technologies showing significant potential and great promise for further investigation, development and application.

Sukitpaneenit and Chung [12] present a comprehensive survey of various membrane materials ranging from polymers, inorganic membranes, and mixed-matrix or hybrid membranes available in the literature for ethanol recovery. A summary of the survey is shown in Fig. 9 of the mentioned paper. According to the mentioned authors, most polymeric membranes reported in previous studies have a relatively low selectivity with a wide range of permeation flux. Silicalite-1 or hydrophobic zeolite membranes exhibit both high selectivity and flux while the pervaporation performance of mixed-matrix or hybrid membranes, which are mostly silicalite-1/PDMS membranes, is spatially scattered in the transition gap between both respective materials. The authors also report results in terms of flux and separation factor for self-developed PVDF/nanosilica dual-layer hollow fibers. They achieved the target for the separation factor of 20 at a permeation flux of 1.1 kg/(m2 h) for a 5 wt.% ethanol feed solution at 50 °C.

In this context, the screening of hydrophobic membranes based on limited information is critical given that the selection task is often costly in time and resources. The product between flux and selectivity appears as the most obvious way to assess the performance of a given hydrophobic membrane. However, in order to fully understand the long-term performance in an integrated system, the analysis must be enhanced by incorporating information about the membrane stability and the influence of fermentation by-products on the separation of ethanol from water for long term experimental runs of a pervaporation module coupled to a laboratory bioreactor operated in a continuous fashion [4]. This is a costly and time-consuming task that should be reserved only for a limited number of membranes.

Several authors have been investigating the influence of fermentation by-products on flux and selectivity of different hydrophobic membranes. Chovau et al. [6] found, for example, that weak acids rendered the Pervap 4060 membrane from Sulzer Chemtech (Switzerland) more hydrophilic, resulting in an increase of water flux up to 48% and a reduction in ethanol permeate

concentration up to 20% with respect to values achieved for a mixture solely composed by ethanol (5 wt.%) and water. The authors also found that even when the addition of impermeable components like glycerol and 2,3-butanediol to an ethanol/water mixture influenced the performances of PERVAP 4060 and Pervatech PDMS (Pervatech BV, The Netherlands – PDMS refers to the membrane material, i.e., polydimethyl siloxane) to some extent, the membrane properties were completely restored afterward, when membranes were subjected to pure ethanol/water experiments. After short-term exposure to these components, the membrane behaved the same as if the exposure never occurred. Stutzenstein [13] found for the case of a non-commercial silica filled-PTMSP (poly[1-(trimethylsilyl)-1-propyne]) membrane (Vito, Belgium) that after changing from a mixture containing glycerol, succinic acid, isoamyl alcohol, active amyl alcohol to an ethanol water solution, flux and separation factor were fully restored. Exposed to the multicomponent mixture, the PTMSP membrane suffered reductions up to 42% and 41.3% in overall and ethanol fluxes, respectively. Results of a study of the influence of lignocellulosic biomass fermentation by-products on the performance of the membrane Pervatech PDMS can be found in Gaykawad et al. [10]. The mentioned authors show irreversible flux reductions, by 17–20% compared to the base case (3 wt.% of ethanol in water) for three different fermentation broths. They also tested the membrane performance behavior in presence of furanics and phenolic compounds. They found, for example, that furfural permeated through the PDMS membrane increasing both flux and selectivity with respect to the base case.

Long term stability is an issue for PTMSP membranes and the subject has deserved the attention of many research groups [14–17]. Fadeev et al. [14] investigated the performance of a PTMSP membrane for the separation of a complex fermentation broth. Both flux and selectivity decreased constantly, reaching stable values corresponding to 10% and 50% of the initial ones, respectively. López-Dehesa et al. [17] found a stable operation of PTMSP membranes after an initial rapid flux decrease.

The screening task, understood as the ranking of membranes among a given number of available membranes, is normally done by running pervaporation experiments in a laboratory setup from model solutions with typical broth compositions.

In this paper, we assess the performance of a given hydrophobic membrane from the conceptual design of a hybrid process formed by the hydrophobic membrane itself and the separation train located downstream [8]. To this end, a single pervaporation experiment with a model ethanol–water mixture is needed to estimate the minimum area requirement of the hydrophobic membrane. Short-cut methods [18–20], on the other hand, can be used to estimate the minimum number of stages and reflux ratio of the distillation column. Estimation of the minimum area requirement for a hydrophilic membrane, which is considered to overcome the azeotropic composition, requires the integration of a spatially one-dimensional isothermal mass transfer model of the unit [21] until the desired biofuel purity is achieved in the corresponding retentate stream. The idea behind the approach is that the performance of a given membrane must be measured taking into account the overall hybrid process given that the hydrophobic membrane itself performs only a part of the desired separation [22]. The hybrid process is then assessed on the basis of a cost estimate using the minimum membrane areas of the two membrane units together with minimum number of stages and minimum reflux ratio of the distillation column among other structural and operating variables.

The outcome allows for the screening of pervaporation membranes, and yields valuable insights into the nature of the process as well as the constraints that a hybrid process may face. Membranes can be assessed based on their overall process performance by this method; only the subset of membranes presenting the best economic figures can be considered for a further analysis.

2. The screening approach

The performance separation index (PSI) for pervaporation is defined in terms of flux and either separation factor ($\alpha_{i,j}$) [6,23] or enrichment factor ($\beta_{i,j}$) [6] in order to reflect the tradeoff between these variables. Table 1 shows the different definitions of PSI valid for either a binary or a multicomponent mixture. The calculation of the performance index requires at least experimentation for a feed with an ethanol concentration similar to that expected in the hot wine stream leaving a fermentation unit coupled to a hydrophobic membrane. In this study, we consider that the concentration achieved in the stirred-tank fermentor is 6 wt.% ethanol, which corresponds to a volumetric productivity of alcohol amounting 6.8 kg/(m^3 h) [24]. The main advantages of this screening procedure are its inherent simplicity and the feedback to membrane developers since the membrane performance in all studied cases must be explained in terms of both operating conditions and membrane characteristics.

Focusing the attention only on the performance of the membrane in a single point without considering its influence in the overall process could lead to a suboptimal choice given that, as mentioned above, the membrane itself forms only a part of the desired separation. Therefore, not only the membrane unit but also the separation train downstream must be considered [22]. Ideally, investment and operation costs of the overall process should be estimated for each membrane option. To this end, rough estimations of equipment sizing and costing must be at hand [8]. The performance of a given membrane can then be measured from economic figures like its contribution to the overall cost per liter of bioethanol.

The conceptual design of the hybrid process shown in Fig. 1a will be used as a screening tool for hydrophobic membranes. The final dehydration step is performed by a pervaporation unit using a hydrophilic membrane to achieve high purity bioethanol in the retentate stream leaving the unit. The permeate stream P^+, containing a low amount of alcohol, is first condensed and then recycled to the distillation column for further processing. In a similar way, the permeate stream P^- leaving the hydrophobic unit must be condensed. For the sake of simplicity, only the vacuum-refrigeration system corresponding to the hydrophobic unit is shown in Fig. 1b.

In order to calculate investment and operating costs for each alternative, the minimum membrane area for each membrane in Fig. 1a and the minimum energy demand of the distillation unit must be properly estimated from shortcut methods.

While flux and selectivity data from a single experiment corresponding to a hydrophobic membrane is the only requisite to estimate the minimum membrane area necessary to achieve a given separation [8], at least a semi-empirical mass transfer model is needed to calculate the surface area of the hydrophilic membrane, as will be explained later [21,25]. Pinch analysis is a useful

Table 1
Common definitions for the performance separation index in terms of either selectivity or enrichment factor [6]. Superscripts P and F stand for permeate and feed, respectively. [PSI] = g/(m^2 h).

	Performance separation index	**Separation** or enrichment factor
Binary mixture	PSI_B = Overall flux $*$ ($\alpha-1$)	$\alpha = (y_{EtOH}{}^P/y_W^P)/(x_{EtOH}{}^F/x_W^F)$
Multicomponent mixture	PSI_M = Overall flux $*$ β	$\beta = y_{EtOH}{}^P/x_{EtOH}{}^F$

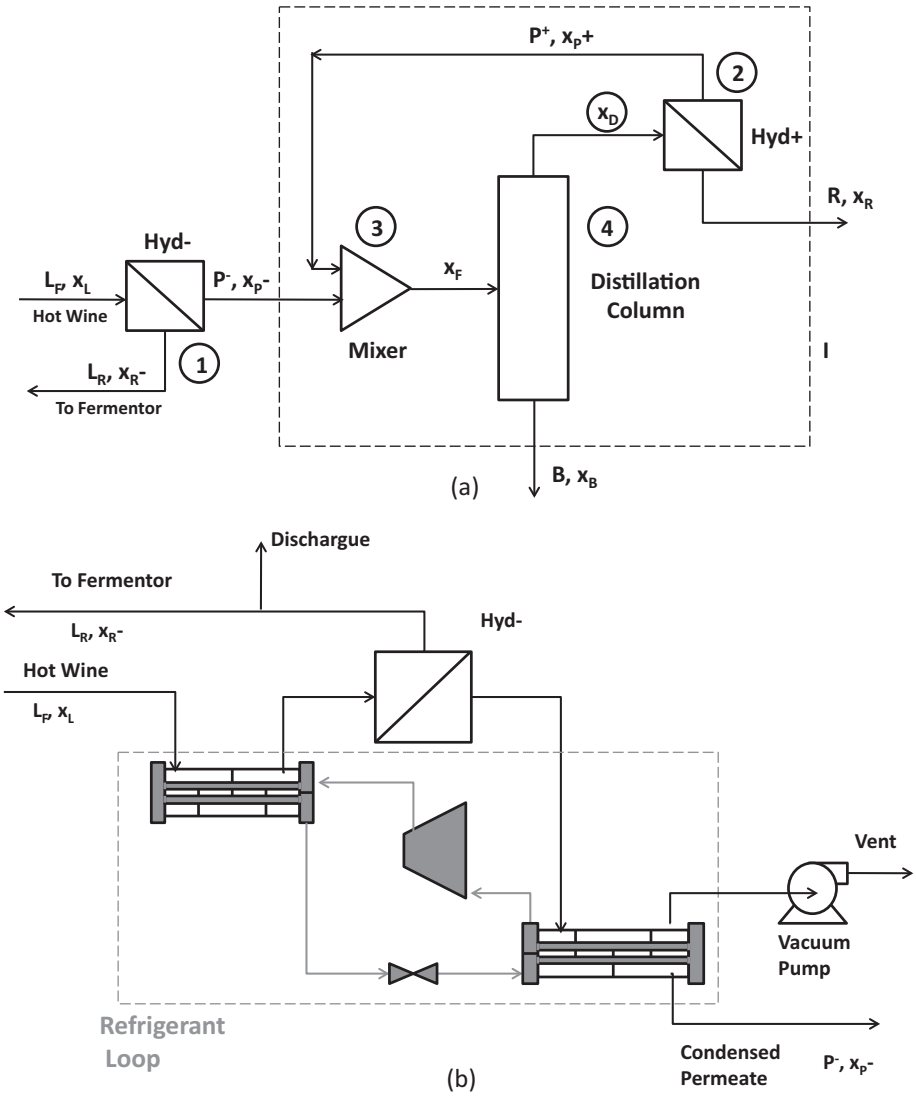

Fig. 1. (a) Flowsheet corresponding to the hybrid process. The distillate composition is the optimization variable. Arabic numbers represent the sequence of design calculations to be followed in order to solve the entire flowsheet without iteration. (b) Vacuum-refrigeration system with heat integration corresponding to the hydrophobic unit.

tool to cope with minimum energy demand calculations for distillation units [20,26,27].

Calculation of the number of stages of a distillation column for a given separation is a challenging task; however, this task is straightforward when assuming a hot wine formed by a binary mixture ethanol–water. In such a case, the number of stages needed for a given separation and reflux ratio can be estimated resorting to the well-known McCabe–Thiele diagram [18]. This assumption has an additional benefit, because for a given value of the distillate mole fraction, the entire flowsheet can be solved without iteration following the sequence of evaluation steps shown in Fig. 1a; i.e., by designing each unit as a standalone process from shortcuts. The search of the optimum flowsheet is easily accomplished by parametrically varying the distillate composition, which in turn is the main optimization variable. Otherwise, a rigorous mixed-integer nonlinear programming (MINLP) optimization of the entire flowsheet should be executed to determine the best alternative [28]. Sosa and Espinosa [29] showed, for the case of isopropyl alcohol dehydration, that the search of a quasi-optimum design with the aid of conceptual models for each unit operation has an advantage with respect to rigorous optimization models. While the use of either a distillation column or a stripper comes up naturally from the design of the distillation unit within the conceptual modeling approach, these alternative process configurations are very difficult to be foreseen when implementing a rigorous optimization approach. It is clear from the mentioned study, that solving that kind of problems should require either a MINLP [30,31] or a disjunctive programming approach [32] in order to capture all the possible process configurations.

Finally, the vacuum-refrigeration system must be modeled in order to include the trade-off between membrane and condensation costs by considering the permeate vacuum as an optimization variable. We consider a system formed by a vacuum pump and a refrigeration cycle to condensate the permeate stream leaving the hydrophilic membrane. The performance of each hydrophobic membrane is assessed by estimating investment cost of the module from the corresponding minimum area requirement. Economic figures for hydrophobic membranes also include the costs of the vacuum-refrigeration system but calculations are performed at the permeate pressure corresponding to the experimental task.

To the best of our knowledge, we are the first in considering the conceptual design of a process comprising two pervaporation units and a distillation column placed in between with a level of detail

that allows for the screening of hydrophobic membranes. The method is not only based on conceptual models for each unit of the hybrid process but also requires dedicated experimental data. This work also aims to improve the representation of the process by incorporating the models corresponding to the vacuum-refrigeration units attached to each membrane into the conceptual design methodology. Relevant contributions in this field are summarized in the review paper written by Skiborowski et al. [21].

3. Problem statement

Two membrane materials have been thoroughly studied for the purpose of recovering organic compounds from water by pervaporation: poly (dimethyl siloxane) and poly[1-(trimethylsilyl)-1-propyne]; PDMS [6,33] and PTMSP [14,34,35], respectively. A thorough analysis on membrane materials for alcohol recovery by pervaporation is carried out by Vane [9].

The main objective of this work is to incorporate the conceptual design approach for supporting the screening of pervaporation membranes for alcohol recovery from fermentation broths. The methodology is demonstrated by considering three different hydrophobic membranes; namely, PERVAP 4060 (Sulzer Chemtech, Switzerland), Pervatech PDMS (Pervatech BV, The Netherlands) and a non-commercial silica filled-PTMSP membrane (Vito, Belgium). These membranes were selected in view of their known performance in the specific application of bioethanol production; it should be noted, however, that while the Sulzer and Pervatech membranes are easily available even at large surface areas, the PTMSP membrane is still in the stage of development and at present not yet applicable for large-scale processes. The hydrophilic membrane MOL 1140 is selected for the dehydration step but other good dehydration membranes could also be considered [36,37].

The membrane performance is assessed in terms of the pervaporation separation index (PSI) and economic figures (U$S/liter) of the hybrid purification process comprising two pervaporation units and a distillation column placed between these units, as shown in Fig. 1a. Results correspond to a feed to the process solely composed by a binary mixture ethanol–water (6 wt.% ethanol) and a plant capacity of 24 million liters bioethanol/yr with a purity equal or higher than 99.8 wt.%.

4. Performance separation index calculation from single experimental data points

Assessment of the technical and economical feasibility of a membrane process requires the determination of values for two relevant membrane properties: selectivity and efficiency. While selectivity is related to the membrane capability to separate two components from a mixture, efficiency is defined as the permeate flux to be achieved under given operating conditions [38].

An important aspect to be understood is that selectivity is a key property since a low selectivity normally leads to a multistage process, which in most cases is not competitive with state-of-the-art processes. A lower efficiency, on the other hand, can be compensated with an increase in the membrane area [38].

A typical way to combine both properties into a single performance index is by multiplying the membrane flux (g/(m^2 h)) by the separation factor α defined in Table 1 in terms of either mass or molar fractions in the feed and permeate streams. For multicomponent mixtures, the enrichment factor β is more appropriate since it allows to investigate the influence of other components (i.e., trace components) in the enrichment of the key component (ethanol in this case) in the permeate in comparison to its concentration in the retentate stream. The performance separation index gives a proper description of the tradeoff observed in most polymeric membranes; that is, a flux increase is typically combined with a decrease in the separation factor [39].

Table 2
Pervaporation Separation Index (PSI) for three available membranes. Feed ethanol concentration in the model ethanol–water mixture: 6 wt.%; operation temperature: 30 °C.

	PERVAP 4060[a]	Pervatech PDMS[a]	Vito PTMSP[b]
Flux (g/(m^2 h))	557	926	2667
Ethanol in permeate (wt.%)	36.5	24.3	29.4
Separation factor	9.00	5.03	6.52
PSI (g/(m^2 h))	4459	3731	14,733

[a] Sosa [40].
[b] Stutzenstein [13].

Table 2 shows fluxes and compositions for the three selected hydrophobic membranes. Both the **separation** factor and PSI are shown for each membrane. Details of the experimental setup can be found in Chovau et al. [6]. Performances of PERVAP 4060 and Pervatech PDMS are comparable to each other. The flux increase of Pervatech PDMS with respect to that of PERVAP 4060 is combined with a decrease in the selectivity factor. The highest performance is achieved by the PTMSP mainly due to its high flux combined with a selectivity factor in between those of the other two membranes considered. The values for this membrane [13] were obtained from a 40 h experiment, which is about the time for stabilization of such membranes according with earlier findings [17].

5. Conceptual models for the pervaporation membranes

Prior to estimating the performance of the three hydrophobic membranes considered in this study from economic figures corresponding to the hybrid process shown in Fig. 1a, it is necessary to revisit the advances achieved in the field of conceptual modeling of pervaporation membranes.

In the typical plate and frame arrangement of a staged pervaporation process a heat exchanger is placed either after a constant temperature drop of the liquid mixture or a constant membrane area. The decrease in the temperature, which results in a decrease of the driving force for the permeation process, is due to the change of state of the permeating components, which take their vaporization heat from the retentate liquid. An additional drop in the driving force for the separation is caused by a concentration decrease of the preferentially permeating component along the retentate side of the module [38]. The concepts above can be visualized in Fig. 2 (Sosa and Espinosa, [29]) by analyzing the variation across the membrane of the retentate temperature, the permeate flux and the composition in the retentate side of the preferentially permeating component. The arrangement comprises five modules of 15 m^2 each, which are needed to dehydrate isopropyl alcohol to a purity of 99.7 wt.%. Along each module, the lowering in the temperature and the molar fraction of water are responsible for the decrease in the overall permeate flux. This tendency is partially tempered by reheating the retentate stream each time it leaves a module. It is a normal practice to reheat the retentate up to a temperature value near the maximum operation temperature of the membrane material.

From the analysis above it is clear that there are two ways to maintain the driving force at its maximum value: (i) by operating the unit at the maximum working temperature of the membrane material, (ii) by avoiding the composition decrease of the preferentially permeating component in the retentate. The achievement of these conditions, whenever possible, under limiting operating conditions for both hydrophobic and hydrophilic membranes will lead to the concept of minimum membrane area.

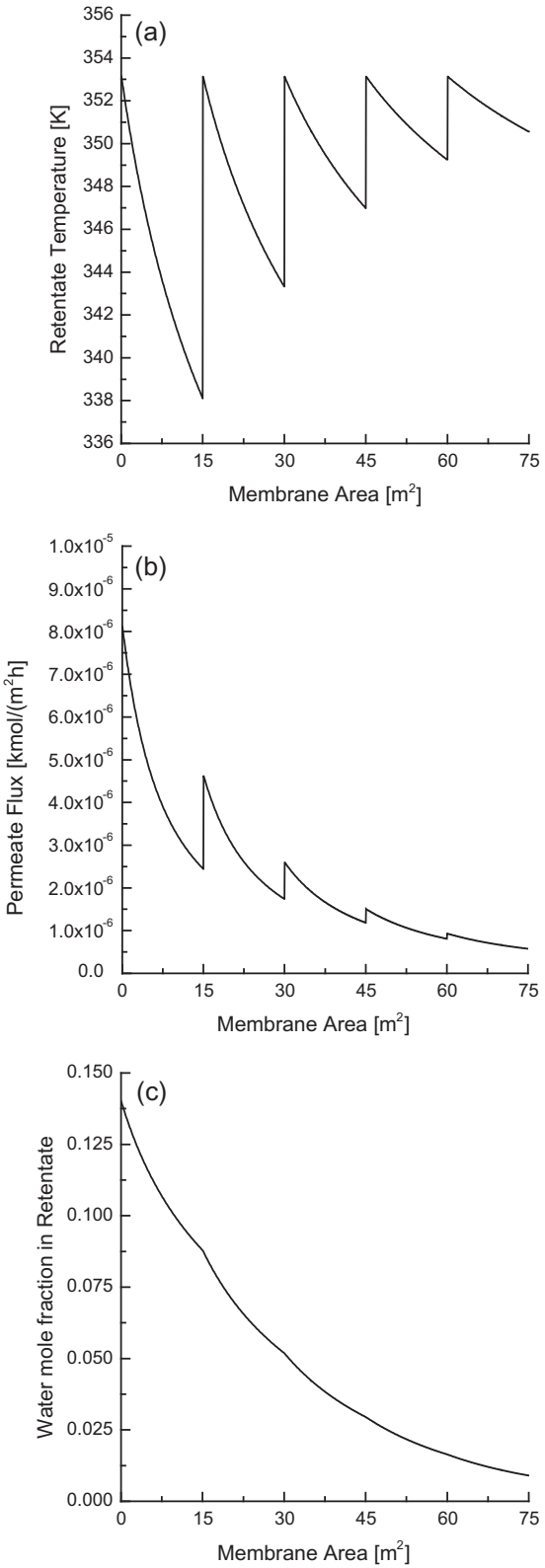

Fig. 2. Variation across the membrane of (a) retentate temperature, (b) permeate flux and, (c) water mole fraction in the retentate side. Feed flow rate: 3.73 kmol/h, feed mole fraction: 0.86, maximum operation temperature: 80 °C, permeate pressure: 1.52 kPa. Unit composed by 5 modules of 15 m^2 each arranged in series.

5.1. Hydrophobic membranes

According to the values presented in Table 2, high concentrations of ethanol in the permeate stream can be achieved by coupling the fermentation unit to pervaporation. As either a decrease in the operating temperature or retentate composition will lead to a decrease in the driving force for separation, a limiting operation condition of an infinite flow rate of the recirculation stream (retentate) between the pervaporation unit and the fermentation unit will maintain the driving force at its maximum feasible value giving rise to an operation with minimum membrane area requirements. In other words, temperature and retentate composition remain unchanged through the membrane unit.

In this case, the selected temperature should be that of the fermentation in order to not to damage the yeast cells. This constraint can be eliminated by adopting more complex arrangements like using microfiltration to separate cells before the hot wine enters the pervaporation unit. Bearing in mind the concepts above, the minimum membrane area can be calculated from the ratio between the ethanol flow rate corresponding to a plant processing 24 million liters/yr of biofuel (kg/h) and the ethanol flux through the membrane (kg/(m^2 h)). This value constitutes a lower bound for the actual membrane area (see Fig. 5 in Bausa and Marquardt, [25]).

According to Melin and Rautenbach [38], there is a barrier which limits the use of hydrophobic pervaporation to a small number of successful examples. This barrier is formed by low permeate flows leading to high membrane area requirements and the high cost involved in the condensation of the permeate stream that frequently must be achieved with the aid of a refrigeration cycle. The high values for membrane areas and condensation duties shown in Table 3 for each case support this claim.

5.2. Hydrophilic membranes

In a similar way to the application of 2-propanol dehydration shown in Fig. 2, the water concentration will decrease along the module in order to allow a high purity ethanol stream to be achieved in the retentate stream leaving the pervaporation unit (x_R in Fig. 1a). As pointed out by Bausa and Marquardt [25], a maximum driving force can be achieved by maintaining the operating temperature at its maximum value by means of an infinite number of heat exchangers. Therefore, the retentate temperature remains unchanged through the hydrophilic membrane but the composition does not.

From this limiting condition, the minimum membrane area can be calculated by integrating a spatially one-dimensional isothermal model of the unit involving a semi-empirical local flux model accounting for the mass transfer through the membrane [21]. In this study, we adopted the model developed by Vier [41] for the membrane MOL 1140 (Eqs. (2)–(5) and parameters given in Table 4). Eq. (1) represents the mass balance around a differential area element of the membrane unit. Subindexes 1 and 2 refer to ethanol and water, respectively. While vapor pressures of pure

Table 3
Minimum area and condensation duty requirements for the three membranes under study. Feed ethanol concentration: 6 wt.%; operation temperature: 30 °C. P^- stands for permeate stream leaving the hydrophobic membrane unit.

	PERVAP 4060	Pervatech PDMS	Vito PTMSP
Flux (g/(m^2 h))	557	926	2667
Ethanol in permeate (wt.%)	36.5	24.3	29.4
$P^-_{Ethanol}$ (kg/h) (overall mass balance)	2368.65	2368.65	2368.65
P^-_{Water} (kg/h)	4120.80	7378.88	5687.98
$P^-_{Overall}$ (kg/h)	6489.45	9747.53	8056.63
Minimum membrane area (m^2)	11,651	10,526	3021
Condensation duty (kW)	3698	6090	4851

Table 4
Parameters corresponding to the mass transfer model of the membrane MOL 1140, a PVA/PAN membrane developed by GFT, Germany, in 1995 (Vier, [41]).

Parameter	Ethanol (1)	Water (2)
c_i	–	0.0011
α_i	–	0.0686
N_i	3.8393	0.0876
E_i/R (K)	6064	5888
T_0 (K)	363.15	363.15
m_i^0 (kg/(m^2 h))	0.0429	5.253
M_i (kg/kmol)	46	18

components are calculated from the Antoine equation, the Wilson equation is used to calculate activity coefficients. Parameters for these equations were extracted from ASPEN Hysys database [42].

$$d[Lx_i] = -J^{mol}_{i,T_{max}}\,dA \tag{1}$$

$$J_1^{mol} = \frac{m_1^0}{M_1} exp\left(N_1 x_1 + \frac{E_{a,1}}{\boldsymbol{R}}\left(\frac{1}{T_0} - \frac{1}{T}\right)\right)(\gamma_1 x_1 - a_{1,p}) \tag{2}$$

$$J_2^{mol} = \frac{m_2^0}{M_2} exp\left(N_2 x_2 + \frac{E_{a,2}}{\boldsymbol{R}}\left(\frac{1}{T_0} - \frac{1}{T}\right)\right)\left(c_2(a_{2,p} - a_{2,p}^2)\right)^{\alpha_2}(\gamma_2 x_2 - a_{2,p}) \tag{3}$$

$$a_{i,p} = \frac{y_i P_p}{P_i^0} \tag{4}$$

$$y_i = \frac{J_i^{mol}}{\sum_j J_j^{mol}} \tag{5}$$

The main model assumptions are: (i) negligible pressure-drop along either side of the membrane surface, (ii) plug-flow along the retentate side of the membrane, (iii) cross-flow along the permeate side of the membrane. In case of a detailed design, mass transport phenomena under non-isothermal and non-stationary conditions must be taken into account [43].

It must be emphasized that once the operating temperature is set at a value near the maximum working temperature of the membrane material (i.e., 90 °C), component fluxes are a function of retentate mole fractions. Therefore, flux and selectivity vary along the membrane module. From given values of distillate flow rate and composition, integration of Eq. (1) together with Eqs. (2)–(5), must be performed until the composition of the retentate achieves a purity above 99.8 wt.%. The calculated area (independent variable in Eq. (1)) represents the minimum membrane area needed to reach the given separation. Retentate and permeate flow rates, and permeate composition are also results obtained from the unit model.

As stated above, in order to calculate the minimum membrane area, both the distillate flow rate and mole fraction must be known or specified. However, from the mass balance around envelope I of Fig. 1a, only the retentate flow rate (24 million liter per year) and mass fraction (99.8 wt.%) are known since they correspond to overall plant specifications. To overcome this problem, Bausa and Marquardt [20] proposed to integrate the unit model for a given value of the distillate mole fraction in the following way:

Step 1. Integrate Eq. (1) together with Eqs. (2)–(5) for a normalized value of the feed flow rate (i.e., 1 kmol/h) with mole fraction $\boldsymbol{x_D}$ (optimization variable), until the retentate composition $\boldsymbol{x_R}$ specified at the design level is achieved;

Table 5
Minimum area and condensation duty requirements for membrane MOL 1140 (GFT, Germany). Overall mass balance is also shown. T = 90 °C, P_p = 2.026 kPa. Values for design and optimization variables are shown in bold.

MOL 1140	
Overall Mole Balance	
D (kmol/s)	0.018296
x_D (mol/mol)	**0.8**
R (kmol/s)	**0.01463**
x_R (mol/mol)	**0.986**
P^+ (kmol/s)	0.003666
x_{P+} (mol/mol)	0.057691
Minimum membrane area (m^2)	662
Condensation enthalphy (kJ/kmol)	47,280
Condensation duty (kW)	173

Step 2. Calculate the values of the minimum membrane area A_{min}, feed flow rate D and permeate flow rate P^+ from normalized values of area a_{min} and retentate flow rate r obtained in Step 1, and the retentate flow rate R specified at the design level:

$$A_{min} = \frac{R}{r} a_{min} \tag{6}$$

$$P^+ = \frac{R}{r}(1 - r) \tag{7}$$

$$D = \frac{R}{r} \tag{8}$$

Model integration including Eqs. (6)–(8) was performed both in Borland Delphi [44] environment and gPROMS [45] obtaining results with the same degree of accuracy. Table 5 shows input data and results obtained for an example. Input data are the retentate flow rate (0.01463 kmol/s) instead of distillate flow rate and molar composition (0.80), the maximum working temperature (90 °C), the retentate mole fraction (0.986) and the permeate pressure (2.026 kPa). The actual membrane area is a calculated value and it is approximated by multiplying the minimum membrane area by a fixed factor of 1.25. Distillate and permeate flow rates, and permeate composition are also results obtained from the unit model. Note that the factor of 1.25 was obtained by comparing different design cases with a typical temperature drop per module of 10 K with their corresponding minimum membrane area [25]. Sosa and Espinosa [29] also applied successfully this figure to isopropyl alcohol dehydration.

Fig. 3 shows the influence of the distillate mole fraction on the minimum area requirement for different values of the permeate pressure as obtained from integration of the conceptual model. In all cases, the retentate stream achieved the required purity (i.e., 99.8 wt.% in ethanol).

6. Conceptual model for the vacuum-refrigeration system

The vacuum-refrigeration system is formed by a vacuum pump and a refrigeration cycle using propane as refrigerant. The power consumption of the vacuum pump was correlated to pumping speed [46]. The refrigeration cycle considers equations for heat exchangers, a single-stage compressor and a choke valve [47]. Focusing our attention on permeate stream to be recycled to the distillation unit, main input data to model the process are pressure, temperature, composition and flow rate of the permeate stream leaving the hydrophilic membrane and actual membrane area. The vacuum pump, which removes small amounts of non-condensed ethanol–water and the leakage air, is located after the permeate condenser. The main optimization variables of the subsystem are the cooling

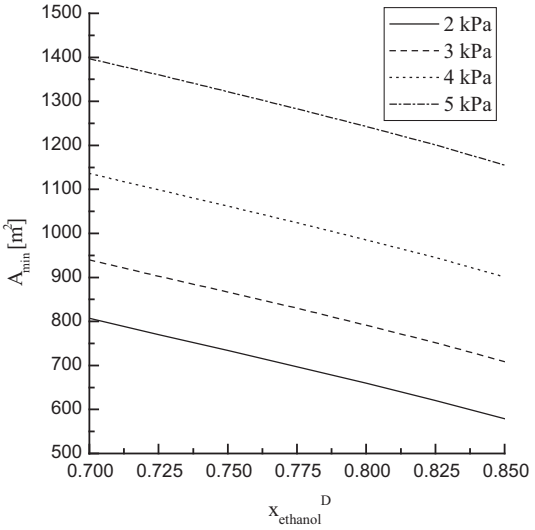

Fig. 3. Minimum membrane area versus ethanol mole fraction in distillate for different values of the permeate pressure. x_R = 0.986, T = 90 °C.

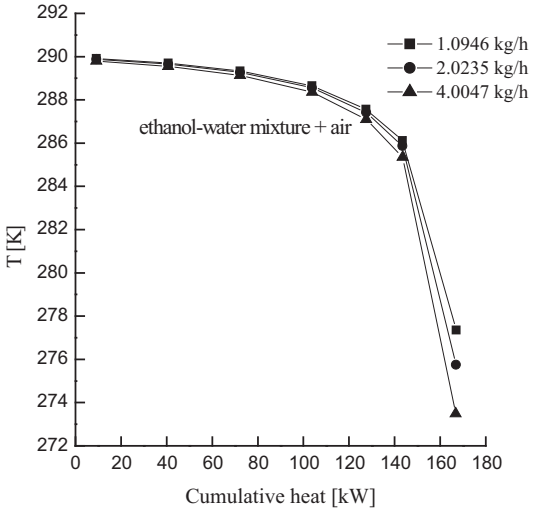

Fig. 4. Heat release curves of the vacuum condenser at the optimum for different air leakage mass flow rates. Input data taken from Table 5.

temperature of the permeate stream and low and high operation pressures of the refrigeration cycle. As emphasized by Fahmy [48], estimation of the flow rate of the leakage air stream in all equipment under vacuum is important to allow a proper design of both the condenser and the vacuum pump.

A quasi-optimal design of this sub-system can be obtained with the aid of rigorous simulation in a process simulator like ASPEN PLUS [42]. However, we decided to model it in MATLAB [49] environment to obtain an optimal design by minimizing the overall annual investment and operation costs of the process. We also add to the objective function a cost accounting for the loss of non-condensed ethanol. In this way, a time-consuming trial-and-error procedure, which does not guarantee finding the optimal solution, is avoided. The MATLAB routine "fmincon", which is a constrained nonlinear optimization algorithm, was used to find the optimal solution.

The main inequality constraints of the model are: minimum approach temperature (ΔT_{min}) in each heat exchanger and a constraint over the lowest cooling temperature in the condenser to avoid ice formation on the cooling surfaces of the vacuum condenser when the freezing point of the permeate mixture is reached. We also add an equality constraint to link the air leakage flow rate to the volume of all equipment under vacuum [50].

In order to improve both the accuracy and the speed of the optimization, we resorted to a fast calculation method for the thermodynamic properties of the refrigerant. Among the methods to speed up calculations of the thermodynamic properties of the refrigerant, we selected the implicit regression and explicit calculation method because it guarantees speed and stability of calculations together with reversibility of estimations [51,52]. This approach to calculate thermodynamic properties was included into the model of the vapor-compression refrigeration cycle. Appendix A shows exemplarily the explicit equation systems used to calculate both the saturation temperature as a function of the saturation pressure and vice versa. The average percent relative deviations between NIST data (National Institute of Standards and Technology, [53]) and calculated data are 0.0001and 0.0011, respectively.

It is noteworthy that the greater the air leakage, the greater the amount of ethanol–water vapor that exits the condenser with the non-condensable air; which in turn increases the size and cost of the vacuum pump. Additionally, the amount of non-condensable gas changes the shape of the heat release curve. Larger air volumes result in larger vacuum condensers and lower effective logarithmic mean temperature differences (LMTDs). Fig. 4 shows cumulative heat release curves corresponding to three different air leakage mass flow rates. All curves begin at the point (0 kW, 363.14 K). Each optimization performed in MATLAB corresponds to a different correlation for the air leakage mass flow rate, which is a function of the volume to be maintained under vacuum and the quality of the seals of the units and ducts. In this work, we adopt the correlation corresponding to seals of high quality [38,50,54]. All calculations were done assuming a negligible pressure drop, which is a valid assumption at the conceptual design level.

Figs. 5 and 6 show the overall annual cost and the ethanol recovery in the condensed permeate versus permeate cooling temperature, respectively. Input data are summarized in Table 5. Fig. 5 shows the typical trade-off between refrigeration and vacuum costs. The optimal cooling temperature $T_{cooling}$ is 277.35 K. For this temperature, the ethanol recovery in the condensed permeate stream is about 95% as shown in Fig. 6. Results shown in these figures were obtained by running the optimization model for different values of the cooling temperature. The same optimum is

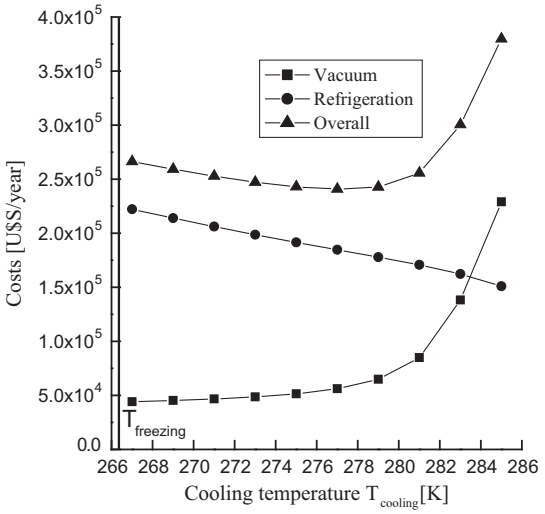

Fig. 5. Trade-off between refrigeration and vacuum costs. Input data taken from Table 5.

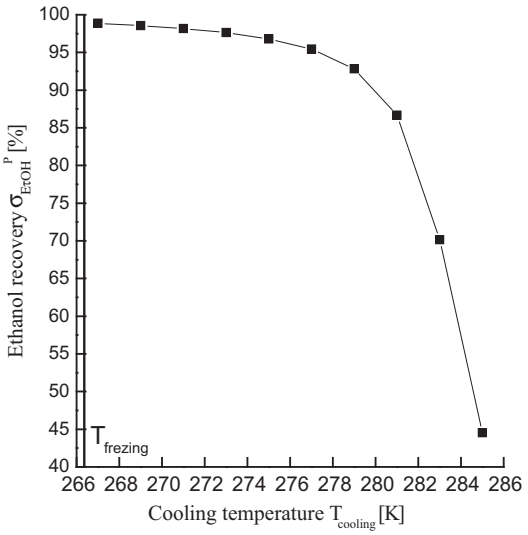

Fig. 6. Ethanol recovery in the condensed permeate versus cooling temperature. Input data taken from Table 5.

Table 6
Optimal design of the refrigeration–vacuum system from input data taken from Table 5. Values for optimization variables are shown in bold.

Cooling temperature $T_{cooling}$ (K)	**277.35**
P_{high} (kPa)	**1907.17**
P_{low} (kPa)	**462.97**
Vacuum condenser area (m^2)	13.92
Propane condenser area (m^2)	17.00
Compressor duty (kW)	54.60
Vacuum pump duty (kW)	3.81
Propane mass flow rate (kg/h)	2440
Actual volume flow (m^3/h)	138.07

obtained by letting free $T_{cooling}$ as an optimization variable. Table 6 shows the results obtained from the conceptual design of the process.

The same model for the vacuum-refrigeration system coupled to each hydrophobic membrane unit was adopted in this work. Due to the high condensation duties reported in Table 3, we assumed a parallel module arrangement of the membrane units to allow using a pump as vacuum technology. This assumption, which is appropriate for the screening procedure, enabled to estimate condensation costs of the permeate streams leaving their corresponding hydrophobic membrane units. As it will be seen in Section 8, condensation costs represent from 38% to 65% of the overall cost of the process comprising a pervaporation unit and the vacuum-refrigeration system.

7. Conceptual model for the distillation column

In order to determine the operation and design variables for feasible columns corresponding to the three flowsheets under analysis, we resorted first to the well-known McCabe–Thiele method [26,27] and then to a rigorous simulation of the unit. The conceptual modeling of each column was performed in DISTIL [55]. Once convergence is achieved at the simulation level, the column diameter can be calculated with the aid of the tray sizing utility incorporated as an Aspen Hysys tool [42]. The feed to each process is obtained by mixing the permeate stream leaving the corresponding hydrophobic membrane with the permeate leaving the hydrophilic membrane MOL 1140. Note that, for a more detailed design, the permeate stream should be fed near the column bottom at a stage with similar ethanol content. However, results obtained at the conceptual design level do not change due to the low permeate flow rate in comparison with that of the feed to the column. Table 7 shows the results achieved. Minimum reflux ratios for the three alternatives are similar to each other even when values of the feed composition vary from 24.3 to 36.5 wt.%.

Table 7
Column designs for the three alternatives studied. x_D = 0.8. Data corresponding to the permeate recycle from the membrane MOL 1140 are given in Table 5.

	PERVAP 4060	Pervatech PDMS	Vito PTMSP
Reboiler duty (kW)	1523	1642	1598
Condenser duty (kW)	1462	1547	1512
Column diameter (m)	0.9144	0.8938	0.9144
Column height (m)	18.90	15.24	15.24
Number of stages	31	25	25
Feed stage	24	17	18
R_{min}	0.84	1.04	0.93
R_{op}	1.08	1.20	1.15

This behavior can be explained by the shape of the vapor–liquid equilibrium curve, which shows an inflexion point. Minimum energy demand for mixtures with an S-shape equilibrium curve is controlled by tangent pinch points.

Fig. 7 depicts graphically the concepts explained above. While the minimum energy demand of the column corresponding to the Pervatech alternative is controlled by a feed type pinch x_P^1, separations with feed composition in the interval (x_N = 35.3 wt.%, x_t = 78.6 wt.%) are controlled by the tangent pinch point x_t.

The separation corresponding to the PERVAP 4060 alternative falls in this case. In Fig. 7 x_N is obtained from the intersection between the operating line of the rectifying section at minimum reflux and the vapor–liquid equilibrium curve, and represents the minimum feed composition for which x_t controls the separation. The minimum reflux ratio of the column corresponding to the PTMSP alternative is in between the other two alternatives with a feed type pinch controlling the separation. The feed pinch for the PTMSP alternative follows the same trend as the reflux ratio.

Finally, as the operating line corresponding to the column design of the PERVAP 4060 alternative approaches the equilibrium curve in the neighborhood of the tangent pinch x_t, this separation demands the highest number of stages to reach the desired separation.

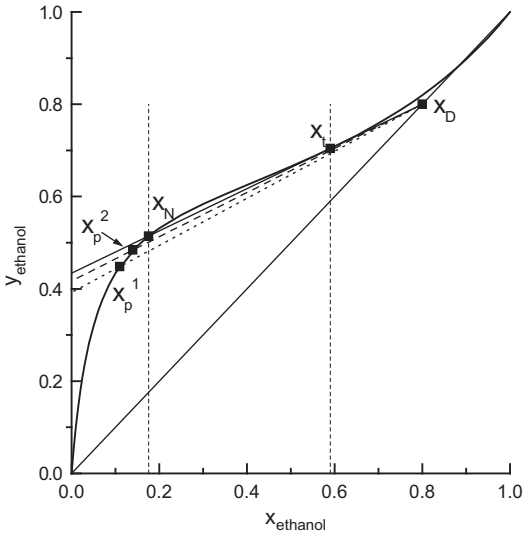

Fig. 7. Minimum reflux for the separations corresponding to the alternatives PERVATECH PDMS, Vito PTMSP and PERVAP 4060. In all cases the distillate mole fraction is 0.8 (molar basis). Controlling pinch points are also shown: X_p^1 for Pervatech PDMS, X_p^2 for Vito PTMSP and X_t for Pervap 4060.

8. Calculation sequence and performance comparison from economic figures

Taking into account that the entire plant mass balance can be calculated from given values of the retentate mole fraction (99.8 wt.% ethanol), and the ethanol mole fraction in the bottom of the distillation column (0.02 wt.%), a degree-of-freedom analysis shows that one degree of freedom remains unspecified. We select the composition of the feed to the hydrophilic membrane unit, which is, in turn, the distillate composition of the main column $\boldsymbol{x_D}$. We also add the corresponding permeate pressure P_P as an additional optimization variable since the vacuum-refrigeration system is also included in the model of the separation train downstream the hydrophobic membrane. Therefore, in order to find an optimum flowsheet for each hydrophobic membrane under study both variables must be parametrically varied within a given interval. The search space for the optimization variables is [0.75, 0.85] for the distillate composition and (2 kPa, 5 kPa) for the permeate pressure, respectively. For each value of the pair ($\boldsymbol{x_D}$, P_P), the design of the overall process must be performed first. Then, the corresponding investment and operation costs can be estimated from a cost model like the methods proposed by Guthrie [56] for the investment costs and by Ullrich and Vasudevan [57] for the operation costs. Installation costs of the membrane module were assumed to be 1816 U$S/m^2 with membrane replacement costs of 144 U$S/m^2 and a membrane lifetime of 3 years.

As shown in Section 5, the area requirements for each hydrophobic membrane can be easily estimated from the overall mass balance and the corresponding data of flux and selectivity. Estimations of the condensation costs must also be provided at least for the pressure adopted in the experimental task (step 0). The search of a cost-effective flowsheet corresponding to the purification train downstream requires, on the other hand, finding quasi-optimal designs for each value of the pair ($\boldsymbol{x_D}$, P_P). This can be accomplished without the need to iterate, even when the flowsheet presents a recycle stream, solving each unit operation as a standalone process. To this end, the following sequence must be followed: (i) hydrophilic membrane unit, (ii) vacuum-refrigeration system, (iii) mixing operation, and (iv) main column.

Step 0: Hydrophobic membrane unit

Fig. 8 shows the overall costs of each hydrophobic membrane studied. Even when the cost of the membrane unit for the PTMSP alternative is about 2.5 times lower than that of the other two alternatives mainly due to its lowest area requirement, the ratio between the overall cost of the Vito PTMSP and the cost of either the Pervatech or Pervap diminishes when costs of the vacuum-refrigeration system are taken into account. Following the trend for the required condensation duties shown in Table 3, the cost of the vacuum-refrigeration system of Pervap PDMS and Pervatech PDMS have the lowest and highest values, respectively. In summary, the cost of the Vito PTMSP is about 1.7 and 1.5 lower than the costs of the Pervatech and Pervap alternatives, respectively. The contribution of each membrane unit to the biofuel cost is then 0.25, 0.37 and 0.43 U$S/liter for Vito PTMSP, Pervap PDMS and Pervatech PDMS, respectively.

Step i, ii, iii and iv: Purification process

Focusing the attention on the downstream process, an interesting result was obtained by maintaining the distillate mole fraction at a constant value. Fig. 9 shows results for a distillate mole fraction of 0.85. For all alternatives analyzed, the optimal permeate pressure was about 1.5 kPa.

The same trend was obtained for other distillate compositions. This behavior can be explained since the optimal value for the permeate pressure is controlled by the trade-off between the costs of the hydrophilic membrane unit and the vacuum-refrigeration system; the costs corresponding to the distillation unit are almost constant due to a controlling tangent pinch. Given that the membrane MOL 1140 is characterized by its low flux and high selectivity, the investment cost of the membrane unit dominates the costs of the system membrane unit/condensation system and therefore, the optimal value for the permeate pressure is the lowest feasible one. For this reason, we adopt 2 kPa as the quasi-optimum value because it was the lowest value for which experimental data were obtained [41]. Results shown in Fig. 10 for the PTMSP membrane support the statements above. Note, however, that these conclusions cannot be extended for the case of a high flux-low selectivity membrane. Moreover, they are not valid for systems in which the column design is not controlled by a tangent pinch.

Fig. 11 shows the results obtained from the parametric variation of the distillate composition for the three alternatives considered. While the optimal distillate mole fraction for Pervatech PDMS and Vito PTMSP is about 0.81, the optimal $\boldsymbol{x_D}$ for Pervap PDMS is about 0.79. The contribution of the purification process to the biofuel cost is 0.058, 0.059 and 0.061 U$S/liter for Pervap PDMS, Vito

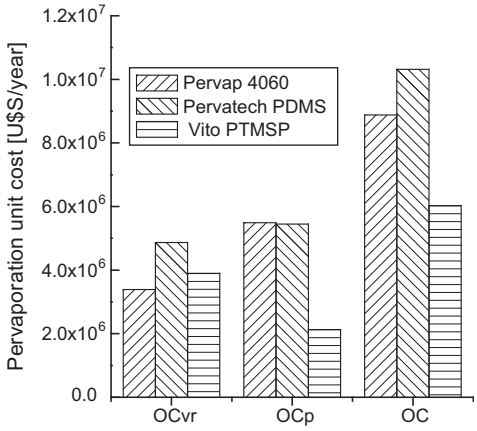

Fig. 8. Annual cost of each hydrophobic unit calculated as the cost of the pervaporation unit (OCp) plus the cost of the vacuum-refrigeration system (OCvr).

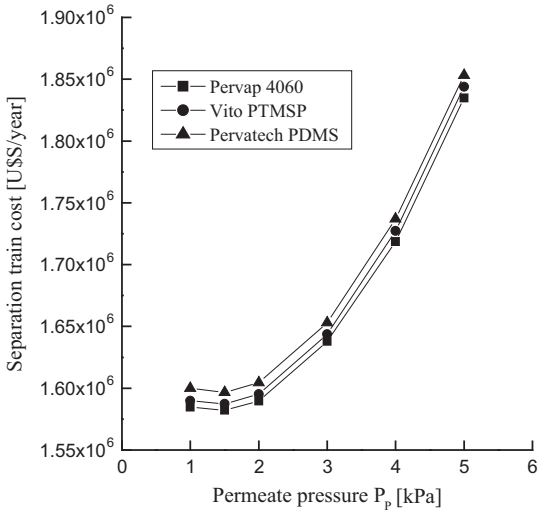

Fig. 9. Overall costs of the separation train versus permeate pressure P_P. All optimizations were performed for a distillate composition $\boldsymbol{x_D}$ = 0.85.

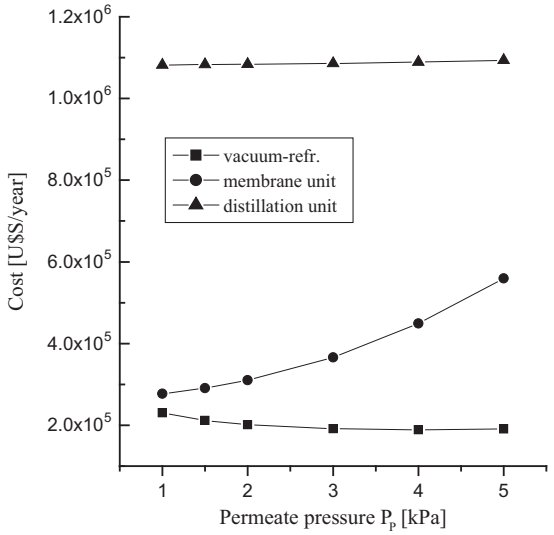

Fig. 10. Annual cost for each unit comprising the downstream process versus permeate pressure $x_D = 0.85$.

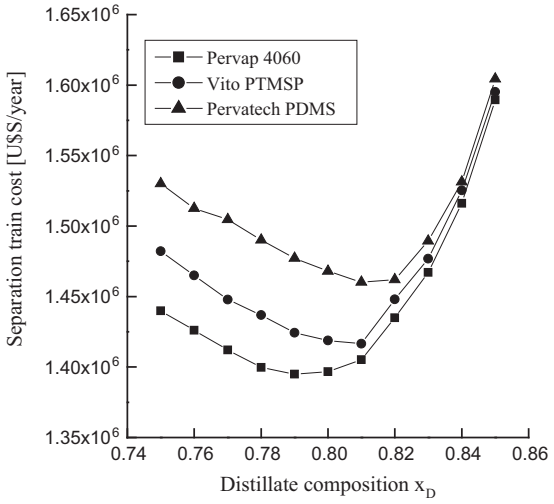

Fig. 11. Overall costs versus distillate composition x_D at $P_p = 2$ kPa.

Table 8
Overall results for the optimal flowsheet.

	Investment and Operating Cost [U$S/year]		
	Pervap 4060	Pervatech PDMS	Vito PTMSP
Purification process	1.395 E6	1.460 E6	1.417 E6
Membrane unit	8.879 E6	10.313 E6	6.030 E6
Overall	10.274 E6	11.733 E6	7.447 E6
Cost per liter [U$S/l]	0.428	0.491	0.310

PTMSP and Pervatech PDMS, respectively. Economic figures for each alternative are summarized in Table 8 including costs obtained in *Step 0*.

9. Model validation and model complexity considerations in the framework of process synthesis

In this section, both a refinement of the model corresponding to the hydrophobic membranes and a brief discussion about model complexity in the framework of process synthesis is presented.

As mentioned in Section 5, the minimum membrane area for each hydrophobic membrane can be estimated from a single experimental point by resorting to the limiting operation condition of an infinite flow rate of the recirculation stream (retentate) between the pervaporation unit and the fermentation unit. As the flow rate of the stream leaving the fermentation unit increases, the decrease in temperature and concentration of the permeating component at the retentate side of the membrane module is reduced. Hence, a higher driving force for permeation is available, which results in a smaller membrane area requirement. For the limiting operating condition of an infinite flow rate, the minimum membrane area is reached. This value is a lower bound for the actual membrane area [25] and can be computed from the ratio between the ethanol flow rate corresponding to a plant processing 24 million liters/yr of bioethanol (kg/h) and the ethanol flux that permeates through the membrane (kg/(m^2 h)) obtained from a single experimental run at a feed composition obtainable in a stirred-tank fermentor.

According to Bausa and Marquardt [25], there is also a minimum flow rate which characterizes the limiting operation at minimum driving force. In this case, the membrane area tends toward infinite.

Thus, the flow rate of the feed to the membrane unit is a degree of freedom which can be used to approach the limiting condition of minimum membrane area with a finite value of feed flow rate.

To check the validity of the conceptual model, simple empirical local flux models for water and ethanol were built for each membrane under study, based on flux and selectivity data obtained at different feed concentrations [13,29]. Thus, it was possible to compute the minimum membrane area in a similar way to that of the hydrophilic membrane by integrating a spatially one-dimensional isothermal model of the unit. Fig. 12 shows the results obtained for each membrane. In the case of the membrane PTMSP, we resorted to short-term experimental data [13]. As will be explained below, the validity of the model remains unchanged. Each point of the curve A_{min} versus $L_F/L_F^{infinite}$ was obtained by integrating Eq. (1) together with the equations for the corresponding empirical local fluxes and Eqs. (6)–(8). The integration proceeds until a given specification for the mass fraction in the retentate stream returning to the fermentation unit; namely x_{R-}, is met. For known values of the composition of the stream fed to the unit x_L (6 wt.% ethanol) and the ethanol flow rate in the permeate stream $P^- x_{P-}$, the model computes values for the flow rates of the feed to the membrane L_F, the recycle stream L_R, and the minimum membrane area A_{min}. Note that in Fig. 12 we use the ratio $L_F/L_F^{infinite}$ in the x-axis with $L_F^{infinite} = 36$ kmol/s. The curves obtained resemble Fig. 5 in Bausa and Marquardt [25] for design cases in which the permeate is the intended product.

From an analysis of Fig. 12, the following conclusions can be drawn for the three membranes considered: (i) the minimum feed flow rate ratio for which the driving force vanishes is about 1.7%, (ii) membrane areas increase rapidly in the prescriptive region, i.e., in the region defined approximately by the interval [1.7%, 3%], (iii) the operating window is relatively narrow, (iv) the lower the membrane area for the limiting operating condition of infinite flow rate, the greater the feed flow rate ratio to achieve a design with a minimum area requirement 1.25 times the corresponding to the asymptotic value, (v) the asymptotic value of the minimum membrane area is a good approximation to assess the membrane performance.

In Fig. 12, the design with a minimum area requirement 1.25 times the corresponding to the lower bound at infinite flow rate is selected as a representative feasible design for a finite value of the ratio $L_F/L_F^{infinite}$. The operation window in all cases is relatively narrow to avoid the limiting operation conditions of infinite membrane area (low values of the feed flow rate) and infinite pumping

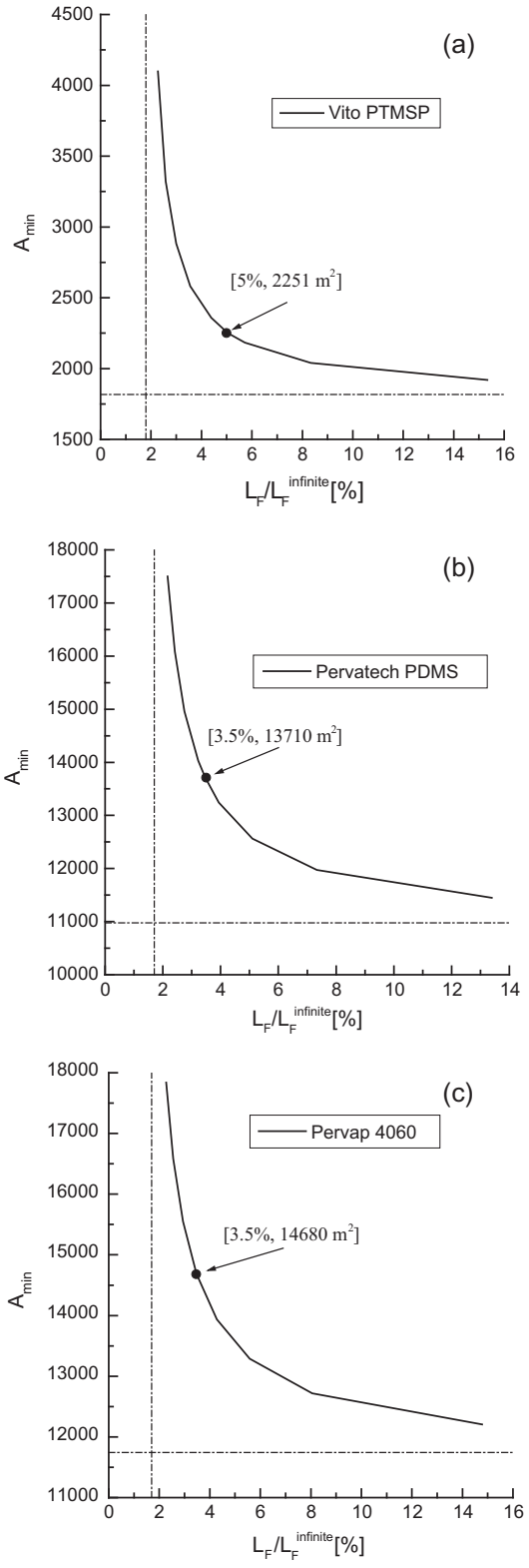

Fig. 12. Minimum membrane area [m^2] as a function of the feed flow rate ratio [%]. The design for a minimum membrane area 1.25 times the asymptotic value is also shown. (a) Vito PTMSP from short-term experiments, (b) Pervatech PDMS, (c) Pervap 4060.

costs (high values of the feed flow rate) and the curves present an asymptotic behavior for the minimum membrane area. Thus, it is clear that the minimum area requirement computed from the limiting operation of infinite flow rate can be used to estimate the membrane performance at a very low cost; i.e., from a single pervaporation experiment.

However, in order to properly evaluate the performance of the three membranes at finite values of the feed flow rate, the design corresponding to a value of the ratio $L_F/L_F^{infinite}$ of 0.05 is chosen. Since the gap between the designs at 3.5% and 5% for both PDMS membranes represents an "enhancement" window with respect to the PTMSP it is possible to predict a lowering in the performance gap of this membrane with respect to the other two analyzed.

To this end, we must estimate the performance of the Vito PTMSP corresponding to the ratio $L_F/L_F^{infinite}$ of 0.05. All curves in Fig. 12 are limited by a common asymptote for the feed flow rate and their own asymptote for the lower bound of the membrane area. Thus, the actual behavior of the PTMSP membrane should be in between of those of the PDMS membranes and the "ideal" performance of the PTMSP estimated from short-term experiments shown in Fig. 12a. In fact, the asymptotic value of the membrane area obtained for this membrane is 3021 m^2 (Table 3), which is above the area requirement of 1817 m^2 predicted from short-term experimental data. This means that the design corresponding to a minimum area requirement of 1.25 times the corresponding to the asymptotic value given in Table 3 (i.e., 3776 m^2) will be achieved for a feed flow rate ratio in the interval [3.5–5%]. We assume for this operating point, a conservative value for $L_F/L_F^{infinite}$ of 0.05. Therefore, the actual behavior of the PTMSP membrane is characterized by the point [5%, 3376 m^2].

Table 9 shows the results obtained from the refined conceptual model. Note that while the minimum membrane area for the Vito PTMSP membrane increases its value from 3021 m^2 (asymptotic value) to 3776 m^2 (+25%), the area increase for the membranes Pervap 4060 and Pervatech PDMS with respect to their corresponding asymptotic values are 15% and 14.5%, respectively. Figs. 13 and 14 show the results obtained for the minimum area and the condensation duty requirements from the models based on the two approaches used.

The contribution of the hybrid process to the overall cost of bioethanol for the alternative PTMSP is now 0.37 U$S/liter (see Table 10), a value that represents an improvement of 29.7% and 48.1% with respect to the alternatives using PERVAP 4060 and Pervatech PDMS. Thus, conclusions about the performance of each membrane remain unchanged.

Table 10 also shows the energy needed to recover ethanol (ENRE index) in MJ/kg ethanol. These values must be compared with the heat of combustion of ethanol; i.e., 30 MJ/kg [9]. The energy required to recover ethanol by pervaporation for the membrane PERVATECH PDMS exceeds the energy of combustion of the recovered ethanol while the energy demand for the Vito PTMSP is barely below 30 MJ/kg. Therefore, the improvement of the energy efficiency of the process through heat integration is mandatory. Table 11 shows the results obtained by integrating the feed to the membrane (cold stream) unit with the refrigerant (hot stream) in the condenser of the refrigeration system (see Fig. 1b). Integration is feasible given that the refrigerant temperature is

Table 9
Minimum membrane area, condensation duty and permeate mass flow rate and composition for the three membranes under study corresponding to a feed flow rate ratio $L_F/L_F^{infinite}$ of 0.05. Values in parenthesis indicate relative percent deviation with respect to values obtained from a single point experiment. In all cases the retentate composition x_R-falls from 6% at infinite flow rate to about 4.4% (−27.2%).

	Pervap 4060	Pervatech PDMS	Vito PTMSP
A_{min} (m^2)	13,399 (+15%)	12,052 (+14.5%)	3776 (+25%)
Condensation duty (kW)	4142 (+12%)	6851 (+12.5%)	5753 (+18.6%)
P^- (kg/h)	7277 (+12.1%)	10,971 (+12.6%)	9556 (+18.6%)
x_{P-} (wt.%)	32.6 (−10.7%)	21.6 (−11.1%)	24.8 (−15.6%)

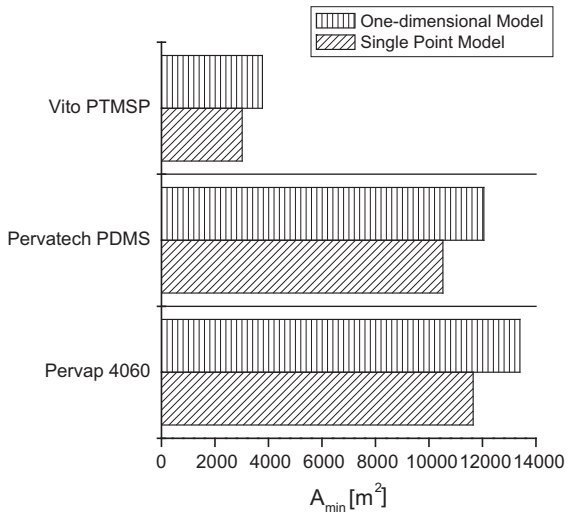

Fig. 13. Minimum area requirements for the membranes under analysis: results obtained from conceptual models based on multiple- and single-point experimental data.

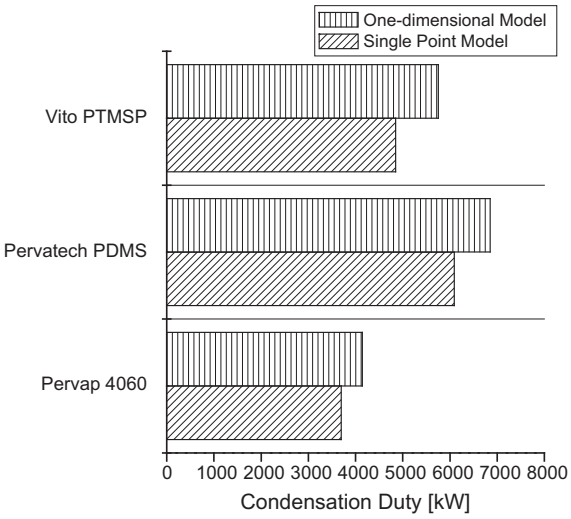

Fig. 14. Condensation duties for the membranes under analysis: results obtained from conceptual models based on multiple- and single-point experimental data.

Table 10
Overall results for the optimal flowsheet obtained from the model refinement of the hydrophobic unit. Values in parenthesis indicate relative percent deviation with respect to values obtained from a single point experiment. Process without heat integration.

	Investment and Operating Cost [U$S/year]		
	Pervap 4060	Pervatech PDMS	Vito PTMSP
Purification process	1.403 E6 (+0.5%)	1.478 E6 (+1.2%)	1.457 E6 (+4.1%)
Membrane unit	10.116 E6 (+13.9%)	11.674 E6 (+13.2%)	7.248 E6 (+20.2%)
Overall	11.519 E6	13.152 E6	8.885 E6
Cost per liter (U$S/l)	0.480 (+12.1%)	0.548 (+11.6%)	0.370 (+19.4%)
Energy to recover ethanol (MJ/kg)	22.1	32.9	28.6

Table 11
Overall results for the optimal flowsheet obtained from the model refinement of the hydrophobic unit. Process with heat integration.

	Investment and Operating Cost [U$S/year]		
	Pervap 4060	Pervatech PDMS	Vito PTMSP
Purification process	1.403 E6	1.478 E6	1.457 E6
Membrane unit	9.125 E6	10.064 E6	5.871 E6
Overall	10.528 E6	11.542 E6	7.328 E6
Cost per liter (U$S/l)	0.439	0.481	0.305
Energy to recover ethanol (MJ/kg)	9.8	12.8	11.5

about 55 °C and the feed to the pervaporation unit must be maintained at 30 °C. Results obtained in terms of ENRE index agree well with those shown in Vane [9]. These values can be also used to make comparisons in terms of energy demand with other alternatives. ENRE values for distillation/hydrophilic pervaporation of 8.7 MJ/kg and for distillation/extractive distillation around 20 MJ/kg can be calculated from simulation results presented in Hoch and Espinosa [58]. As expected, the improvement in the energy efficiency of the process triggers the improvement in both operating and investment costs.

As stated by Vane [9], the integration of pervaporation with fermentation systems will increase fermentor productivity while reducing the amount of water processed in the system. Hence, savings in both investment and operating costs with respect to the conventional process are expected to occur. We developed a cost model for both conventional and hybrid processing facilities mainly by resorting to data from Kwiatkowski et al. [59] and Hoch and Espinosa [58] in order to estimate operating and investment costs for process units different from distillation and membrane operations. Assuming a volumetric productivity in the fermentation unit of the hybrid process of 6.8 kg/(m^3 h) [24], the overall processing costs are in U$S/l 0.665, 0.718, 0.834 and 0.887 for the conventional process, Vito PTMSP, Sulzer Pervap and Pervatech PDMS, respectively. A membrane with flux above 2 kg/(m^2 h) and selectivity above 10 will lead to an overall processing cost which is similar to that of the conventional process. As suggested in Baeyens et al. [60], economic feasibility of the process can be achieved by removing only a part of the total fermentor broth flow rate through the membrane in order to diminish the area requirement of the pervaporaton unit giving rise to a cost-effective process. For the case of the Vito alternative, the hybrid system should continuously remove as permeate about 45% of the overall fermentation unit flow rate. Note however, that these figures should be used as reference values given that the optimal volumetric productivity of the fermentation unit will be obtained in the next selection step; i.e., the performance assessment from long term experimental runs of the hybrid fermentation unit plus a pervaporation unit operated in a closed-loop mode.

Summarizing, the conceptual adopted is suitable for the screening of hydrophobic membranes. However, a more sophisticated model will be necessary for the next selection step; i.e., the performance assessment from long term experimental runs of the continuous process comprised by a pervaporation unit coupled to the fermentation unit. In such a case, the conceptual model must incorporate the influence of a new optimization variable: the feed flow rate to the membrane unit. Considering all the steps of the synthesis of a given process, models must be refined beginning from simple but scientifically well-founded conceptual design models and ending with very complex ones relying on detailed mass and energy balances, rigorous physical property models, and either equilibrium controlled or kinetically limited mass transfer models at every process unit [21].

10. Conclusion

In this manuscript, two ways to assess the performance of hydrophobic membranes were investigated.

The performance separation index (PSI) defined as the product of flux and selectivity factor predicted a remarkable performance for the membrane PTMSP (Vito) in comparison with those corresponding to PERVAP 4060 and Pervatech PDMS. Values reported at 30 °C in Table 2 show that the PSI index for the membrane from Vito that is more than three times the corresponding index for each one of the two other alternatives. However, the application of the conceptual modeling approach to the screening of membranes predicted a rather different situation. As it is shown in the main body of the paper, the contribution of the **heat integrated** hybrid process to the overall cost of bioethanol for the alternative PTMSP is 0.305 U$S/liter, a value that represents an improvement of 43.9% and 57.7% with respect to the alternatives using PERVAP 4060 and Pervatech PDMS, respectively. These figures represent a substantially smaller improvement of the PTMSP membrane with respect to the performance predicted by using the PSI index.

From the analysis of the hybrid process it is concluded that the economic benefits of using the PTMSP membrane mainly arise from the lower investment and operating costs of the hydrophobic pervaporation unit itself. This can be explained as follows: the cost of the purification process downstream is governed by the tangent pinch point in the distillation unit and therefore, the cost of the purification process does not vary significantly among the different alternatives considered. Thus, it is clear that the use of minimum membrane area and condensation duty on the preliminary assessment of the performance of each hydrophobic membrane is much more relevant than the mere use of flux and selectivity data. Furthermore, the proposed approach appropriately captures the main "trade-offs" present in the hybrid process and provides the decision-making process with relevant information like heat integration possibilities.

Finally, it is concluded that the conceptual model adopted is suitable for the screening of hydrophobic membranes from single experimental data. A spatially one-dimensional isothermal model of the pervaporation unit will be necessary, on the other hand, for the next selection step; i.e., the performance assessment from long term experimental runs of the hybrid fermentation unit plus a pervaporation unit operated in a closed-loop mode. From the results obtained, the three hydrophobic membranes analyzed will deserve further analysis. Issues like the influence of fermentation by-products and long-term stability of the membrane properties on separation performance will be then elucidated during process optimization.

Acknowledgments

This work was made in the framework of the following projects: PIP 688 with the financial support from CONICET (Argentina) and FW/11/07 (MINCyT, Argentina and FWO, Belgium). José Espinosa thanks to DAAD (Germany) for equipment donation to CONICET under grant A/03/30363.

Appendix A

A.1. VCRC model and calculation of thermal properties of the refrigerant

According to Ding et al. [52], the requirements for the simulation of a vapor-compression refrigeration cycle (VCRC) should include three main requirements: (1) stability, (2) rapidness and (3) accuracy. These requirements may conflict with each other, and then a compromise has to be made.

To attain this goal a conceptual model of the VCRC was formulated, taking into account super-heating and sub-cooling of the refrigerant (5 K) to guarantee vapor phase entrance to compressor and liquid phase exit of the propane condenser, respectively.

The model of the compressor unit uses a semi-empirical parameter for the polytropic exponent [61] to estimate the outlet temperature of the refrigerant. The mass and energy balances are calculated using thermal properties of the refrigerant.

A multi-node model is adopted for the vacuum condenser (propane evaporator) [51] to allow both a better description of the phase change of condensate through the equipment and a proper estimation of the heat exchange area requirement. The influence of the air leakage on the design of the unit is also considered. The refrigerant condenser model, on the other hand, considers the unit as a whole without dividing the unit into several control volumes.

Furthermore, in order to improve both the accuracy and the speed of the optimization, we resorted to a fast calculation method for the thermodynamic properties of the refrigerant. Among the methods to speed up calculations of the thermodynamic properties of the refrigerant, we selected the implicit regression and explicit calculation method because it guarantees speed and stability of calculations together with reversibility of estimations [51,52].

According to Ding et al. [52] the curve-fitting equations for saturated pressure and temperature takes the form of an implicit cubic equation containing the variables u and v:

$$f(u,v) = u^3 + a_1u^2v + a_2uv^2 + a_3v^3 + a_4u^2 + a_5uv + a_6v^2 + a_7u + a_8v = 0 \quad \text{(A1)}$$

with $v = T - 223.15$ (K) and $u = (P - 70.5685)/300$ (kPa).

Parameters (a_1–a_8) are calculated by regressing data for saturated values of pressure ($Ps = f(Ts)$) and temperature ($Ts = f(Ps)$) in the intervals [70.569, 2689.5 kPa] and [223.14, 345.15 K], respectively. Data were taken from the EOS-based software NIST MINIREFPROP 9.0 [53]. Values of the parameters obtained for propane are given in Table A1.

The implicit equation above can be transformed into a standard cubic equation for each thermal property. The corresponding analytical solutions are given below:

$$P_{sat} = 70.5685 + 300\left(-2\sqrt{Q_1}\cos\left(\frac{\theta_1 - 2\pi}{3}\right) - \left(\frac{B_1}{3A_1}\right)\right) \quad \text{(A2)}$$

$$T_{sat} = 223.15 + \left(\sqrt[3]{-R_2 + \sqrt{\Delta_2}} + \sqrt[3]{-R_2 - \sqrt{\Delta_2}} - \left(\frac{B_2}{3A_2}\right)\right) \quad \text{(A3)}$$

Table A1
Coefficients of implicit equation for saturated pressure and temperature.

a_1	0.222917589304956	a_4	$-1.375565945893193 * 10^2$	a_7	$-3.366785731638515 * 10^3$
a_2	0.058595327896563	a_5	4.717708539558043	a_8	37.823113462413644
a_3	0.005479384424053	a_6	0.667416512093513		

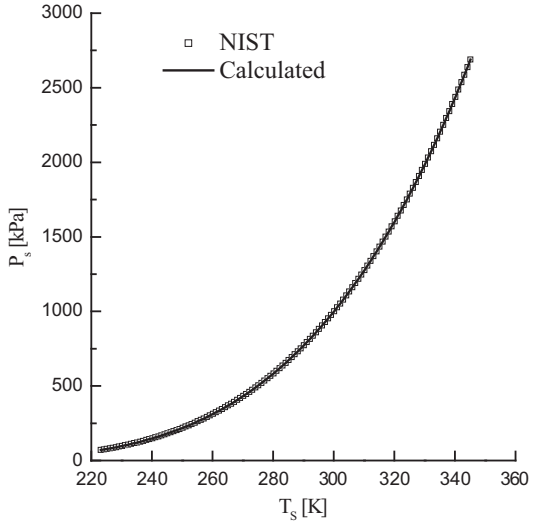

Fig. A1. Saturated propane pressure (kPa) versus temperature (K). Eq. (A2) is used to calculate the saturation pressure.

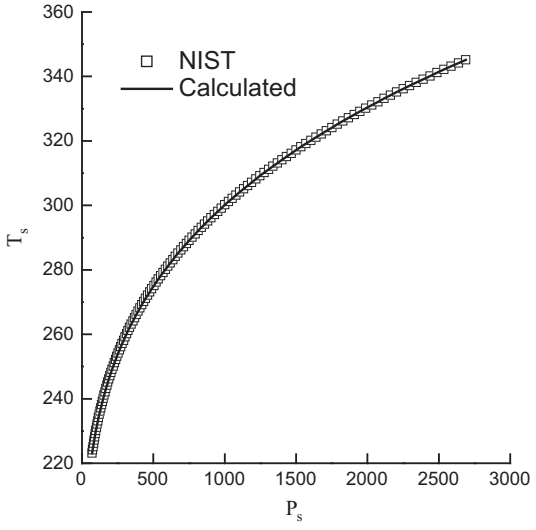

Fig. A2. Saturated propane temperature (K) versus pressure (kPa). Eq. (A3) is used to calculate the saturation temperature.

with

$$Q = \frac{(B/A)^2 - 3(C/A)}{9}$$
$$R = \frac{2(B/A)^3 - 9(C/A)(B/A) + 27(D/A)}{54}$$
$$\Delta = R^2 - Q^3 \qquad \text{(A4-A7)}$$
$$\theta = \arcsin\left(\frac{R}{\sqrt{Q^3}}\right)$$

Coefficients *A*, *B*, *C* and *D*, which are specific for each thermal property, are calculated from the following equations:

Saturated pressure:

$$A_1 = 1$$
$$B_1 = a_1 v + a_4$$
$$C_1 = a_2 v^2 + a_5 v + a_7 \qquad \text{(A8-A11)}$$
$$D_1 = a_3 v^3 + a_6 v^2 + a_8 v$$

Saturated temperature:

$$A_2 = a_3$$
$$B_2 = a_2 u + a_6$$
$$C_2 = a_1 u^2 + a_5 u + a_8 \qquad \text{(A12-A15)}$$
$$D_2 = u^3 + a_4 u^2 + a_7 u$$

Figs. A1 and A2 show both NIST data and calculated values for the saturated pressure and temperature. Excellent agreement is found. The maximum relative deviation found is about 0.0091%.

References

[1] R.C. Binning, R.J. Lee, J.F. Jennings, E.C. Martin, Separation of liquid mixtures by permeation, Ind. Eng. Chem. 53 (1961) 45–49.
[2] G.F. Tusel, H.E.A. Brueschke, Use of pervaporation systems in the chemical industry, Desalination 53 (1985) 327–338.
[3] M. Nomura, T. Bin, S.-I. Nakao, Selective ethanol extraction from fermentation broth using a silicalite membrane, Sep. Purif. Technol. 27 (2002) 59–66.
[4] D.J. O'Brien, L.H. Roth, A.J. McAloon, Ethanol production by continuous fermentation–pervaporation: a preliminary economic analysis, J. Membr. Sci. 166 (2000) 105–111.
[5] L.M. Vane, Separation technologies for the recovery and dehydration of alcohols from fermentation broths, Biofuels Bioprod. Biorefin. 2 (2008) 553–588.
[6] S. Chovau, S. Gaykawad, A.J.J. Straathof, B. Van der Bruggen, Influence of fermentation by-products on the purification of ethanol from water using pervaporation, Bioresour. Technol. 102 (2011) 1669–1674.
[7] N. L Le, Y. Wang, T.-S. Chung, Pebax/POSS mixed matrix membranes for ethanol recovery from aqueous solutions via pervaporation, J. Membr. Sci. 379 (2011) 174–183.
[8] M.A. Sosa, S. Chovau, B. Van der Bruggen, J. Espinosa, Ethanol production from corn contaminated with fumonisins: a preliminary economic analysis including novel processing alternatives, Ind. Eng. Chem. Res. 52 (2013) 7504–7513.
[9] L.M. Vane, A review of pervaporation for product recovery from biomass fermentation processes, J. Chem. Technol. Biotechnol. 80 (2005) 603–629.
[10] S.S. Gaykawad, Y. Zha, P.J. Punt, J.W. van Groenestijn, L.A.M. van der Wielen, A.J.J. Straathof, Pervaporation of ethanol from lignocellulosic fermentation broth, Bioresour. Technol. 129 (2013) 469–476.
[11] H.-J. Huang, S. Ramaswamy, U.W. Tschirner, B.V. Ramarao, A review of separation technologies in current and future biorefineries, Sep. Purif. Technol. 62 (2008) 1–21.
[12] P. Sukitpaneenit, T.-S. Chung, PVDF/nanosilica dual-layer hollow fibers with enhanced selectivity and flux as novel membranes for ethanol recovery, I&EC Res. 51 (2012) 978–993.
[13] P. Stutzenstein, The use of PTMSP membranes for upgrading bioethanol by pervaporation, Master Thesis, University of Natural Resources and Life Sciences, Vienna, Austria, 2013.
[14] A.G. Fadeev, S.S. Kelley, J.D. McMillan, Ya.A. Selinskaya, V.S. Khotimsky, V.V. Volkov, Effect of yeast fermentation by-products on poly[1-(trimethylsilyl)-1-propyne] pervaporative performance, J. Membr. Sci. 214 (2003) 229–238.
[15] L. Starannikova, V. Khodzhaeva, Yu. Yampolskii, Mechanism of aging of poly[1-(trimethylsilyl)-1-propyne] and its effect on gas permeability, J. Membr. Sci. 244 (2004) 183–191.
[16] N. Morlière, C. Vallières, L. Perrin, D. Roizard, Impact of thermal ageing on sorption and diffusion properties of PTMSP, J. Membr. Sci. 270 (2006) 123–131.
[17] C. López-Dehesa, J.A. González-Marcos, J.R. González-Velasco, Pervaporation of 50 wt.% ethanol–water mixtures with poly(1-trimethylsilyl-1-propyne) membranes at high temperatures., J. Appl. Polym. Sci. (2007) 2843–2848.
[18] W.L. McCabe, E.W. Thiele, Graphical design of fractionating columns, Ind. Eng. Chem. 17 (1925) 605–611.
[19] J. Koehler, P. Aguirre, E. Blass, Minimum reflux calculations for nonideal mixtures using the reversible distillation model, Chem. Eng. Sci. 46 (1991) 3007–3021.
[20] J. Bausa, R. von Watzdorf, W. Marquardt, Shortcut methods for nonideal multicomponent distillation: 1. Simple columns, AIChE J. 44 (1998) 2181–2198.
[21] M. Skiborowski, A. Harwardt, W. Marquardt, Conceptual design of distillation-based hybrid separation processes, Annu. Rev. Chem. Biomol. Eng. 4 (2013) 45–68.

[22] A.M. Parvez, P. Luis, T. Ooms, S. Vreysen, P. Vandezande, J. Degrève, B. Van der Bruggen, Separation of ethyl acetate–isooctane mixtures by pervaporation and pervaporation-based hybrid methods, Chem. Eng. J. 210 (2012) 252–262.
[23] W. Kujawski, M. Waczyński, M. Lasota, Pervaporation properties of dense polyamide-6 membranes in separation of water–ethanol mixtures, Sep. Sci. Technol. 31 (1996) 953–963.
[24] D.J. O'Brien, J.C. Craig Jr., Ethanol production in a continuous fermentation/membrane pervaporation system, Appl. Microbiol. Biotechnol. 44 (1996) 699–704.
[25] J. Bausa, W. Marquardt, Shortcut design methods for hybrid membrane/distillation processes for the separation of nonideal multicomponent mixtures, Ind. Eng. Chem. Res. 39 (2000) 1658–1672.
[26] J.G. Stichlmair, J.R. Fair, Distillation: Principles and Practice, Wiley-VCH, New York, 1998.
[27] M.F. Doherty, M.F. Malone, Conceptual design of distillation systems, first ed., McGraw–Hill Chemical Engineering Series, McGraw-Hill, New York, 2001.
[28] W. Marquardt, S. Kossack, K. Kraemer, A framework for the systematic design of hybrid separation processes, Chin. J. Chem. Eng. 16 (2008) 333–342.
[29] M.A. Sosa, J. Espinosa, Feasibility analysis of isopropanol recovery by hybrid distillation/pervaporation process with the aid of conceptual models, Sep. Purif. Technol. 78 (2011) 237–244.
[30] J.A. Caballero, I.E. Grossmann, M. Keyvani, E.S. Lenz, Design of hybrid distillation–vapor membrane separation systems, Ind. Eng. Chem. Res. 48 (2009) (2009) 9151–9162.
[31] M. Skiborowski, K. Kraemer, W. Marquardt (2011), A General Process Design Methodology for Membrane Assisted Hybrid Processes—Deterministic Mixed-Integer Process Optimization, in: EPIC 2011—The 3rd European Process Intensification Conference, pp. 37–45 (Paper 06), IChemE, London.
[32] J.A. Caballero, D. Milan-Yanez, I.E. Grossmann, Rigorous design of distillation columns: integration of disjunctive programming and process simulators, Ind. Eng. Chem. Res. 44 (2005) 6760–6775.
[33] A. Dobrak, A. Figoli, S. Chovau, F. Galiano, S. Simone, I. Vankelecom, E. Drioli, B. Van der Bruggen, Performance of PDMS membranes in pervaporation: effect of silicalite fillers and comparison with SBS membranes, J. Colloids Interface Sci. 346 (1) (2010) 254–264.
[34] J.R. González-Velasco, J.A. González-Marcos, C. López-Dehesa, Pervaporation of ethanol–water mixtures through poly(1-trimethylsilyl-1-propyne) (PTMSP) membranes, Desalination 149 (2002) 61–65.
[35] S. Claes, P. Vandezande, S. Mullens, R. Leysen, K. De Sitter, A. Andersson, et al., High flux composite PTMSP-silica nanohybrid membranes for the pervaporation of ethanol/water mixtures, J. Membr. Sci. 351 (2010) 160–167.
[36] A.M. Urtiaga, E.D. Gorri, I. Ortiz, Pervaporative recovery of isopropanol from industrial effluents, Sep. Purif. Technol. 49 (2006) 245–252.
[37] J. Zuo, Y. Wang, S.P. Sun, T.-S. Chung, Molecular design of thin film composite (TFC) hollow fiber membranes for isopropanol dehydration via pervaporation, J. Membr. Sci. 405–406 (2012) 123–133.
[38] T. Melin, R. Rautenbach, Membranverfahren, Grundlagen der Modul- und Anlagenauslegung, VDI-Buch, Springer, 2007.
[39] T.A. Peters, C.H.S. Poeth, N.E. Benes, H.C.W.M. Buijs, F.F. Vercauteren, J.T.F. Keurentjes, Ceramic-supported thin PVA pervaporation membranes combining high flux and high selectivity; contradicting the flux-selectivity paradigm, J. Membr. Sci. 276 (2006) 42–50.
[40] M.A. Sosa, Síntesis Óptima de Procesos Híbridos con Énfasis en la Recuperación de Solventes y la Producción de Bioetanol para Combustibles, Ph.D. Thesis, Universidad Nacional del Litoral, Argentina, 2014.
[41] J. Vier, Pervaporation azeotroper waessriger und rein organischer Stoffgemische-Verfahrensentwicklung und–integration, Ph.D. Thesis, Institut fuer Verfahrenstechnik, RWTH Aachen, Shaker Verlag, Aachen, Germany, 1995.
[42] Aspen Plus Version 8 User Manual, 2014.
[43] P. Gómez, R. Aldaco, R. Ibáñez, I. Ortiz, Modeling of pervaporation processes controlled by concentration polarization, Comput. Chem. Eng. 31 (2007) 1326–1335.
[44] Borland Delphi 3, Copyright 1997 Borland International, Inc., Scotts Valley, CA, 1997.
[45] gPROMS User Manual, Process Systems Enterprise Ltd., 1998.
[46] Oerlikon Leybold Vacuum Online Catalog. <https://leyboldproducts.oerlikon.com/products/index.aspx>.
[47] J.B. Jensen, S. Skogestad, Optimal operation of simple refrigeration cycles, Comput. Chem. Eng. 31 (2007) 712–721.
[48] A. Fahmy, Membrane Processes for the Dehydration of Organic Compounds, Ph. D. Thesis, University of Hannover, Germany, 2002.
[49] MATLAB 7.4 User Manual, The Mathworks Inc., 2007.
[50] J.V. Gómez, Calculate air leakage values for vacuum systems, Chem. Eng. 98 (1991) (1991) 149.
[51] G.L. Ding, Recent developments in simulation techniques for vapour-compression refrigeration systems, Int. J. Refrig 30 (2007) 1119–1133.
[52] G.L. Ding, Z.G. Wu, K. Wang, M. Fukaya, Extension of the applicable range of the implicit curve-fitting method for refrigerant thermodynamic properties to critical pressure, Int. J. Refrig 30 (2007) 418–432.
[53] NIST REFPROP 9.1, National Institute of Standard and Technology, USA, 2012.
[54] J.R. Couper, W.R. Penney, J.R. Fair, S.M. Walas, Chemical Process Equipment, second ed., Elsevier, Boston, 2010, pp. 119–158.
[55] Distil User Manual; Hyprotech Ltd., Calgary, Canada, 1999.
[56] W.D. Seider, J.D. Seader, D.R. Lewin, Product and Process Design Principles: Synthesis, Analysis, and Evaluation, second ed., Wiley, 2004.
[57] G.D. Ulrich, P.T. Vasudevan, How to estimate utility costs, Chem. Eng. (2006) 66–69.
[58] P.M. Hoch, J. Espinosa, Conceptual design and simulation tools applied to the evolutionary optimization of a bioethanol purification plant, Ind. Eng. Chem. Res. 47 (19) (2008) 7381–7389.
[59] J.R. Kwiatkowski, A.J. McAloon, F. Taylor, D.B. Johnston, Modeling the process and costs of fuel ethanol production by the corn dry-grind process, Ind. Crops Prod. 23 (2006) 288–296.
[60] J. Baeyens, Q. Kang, L. Appels, R. Dewil, Y. Lv, T. Tan, Challenges and opportunities in improving the production of bio-ethanol, Prog. Energy Combust. Sci. 47 (2015) 60–88.
[61] J.R. Lenz, Polytropic Exponents for Common Refrigerants. International Compressor Engineering Conference, 2002. Paper 1528. <http://docs.lib.purdue.edu/icec/1528/>.